Contact Resistances in Spot Welding

Various electrodes were tested to determine the effect of surface condition on contact resistance

BY P. H. THORNTON, A. R. KRAUSE AND R. G. DAVIES

ABSTRACT. The contact resistance of several aluminum alloys with different surface conditions was measured as a function of the applied current and under different applied loads. The magnitude of the contact resistance varied over a wide range of values, depending upon load and surface condition. Usually the contact resistance decreased with an increase in load, but if a surface lubricant was present, an increase in resistance was observed. Extensive plastic deformation occurred under the loading conditions imposed by the electrode tips. A cup and cone profile was found at the contact region of the faying surface after unloading. Under slowly varying currents, ~1 A/s, electrical breakdown effects were observed when the potential across the surfaces was ~0.2 V. The nature of the change was ascribed to metallic conduction and local fusion rather than oxide film breakdown. Under rapidly varying currents, ~10^7 A/s, typical of a spot welding operation, the contact resistance was found to decrease to ~20 μΩ within the first quarter cycle of weld current, irrespective of the initial surface condition of the aluminum alloy. Continued weld current inputs caused a further decrease in the contact resistance to ~10 μΩ. It is concluded that the results of contact resistance tests may be influenced by the test procedure if large currents are used that develop a significant potential difference, >0.2 V, across the interface.

P. H. THORNTON, A. R. KRAUSE AND R. G. DAVIES are with the Research Laboratories, Ford Motor Co., Dearborn, Mich.

Introduction

The metallic contact that occurs between two metal electrodes when placed together actually occurs over only a few microscopically small areas. Current flow through these areas thus is constricted, giving rise to a constriction resistance, R_c,

$$R_c = \rho/d \tag{1}$$

where ρ is the electrical resistivity and d is the diameter of the microscopic contact area (Ref. 1). Generally, even a clean metal surface is tarnished. This surface film may be composed of compounds besides oxide, and it may be conducting, semiconducting or insulating, depending upon the thickness of the film. It can contribute to the resistance of the electrical contact because it decreases the probability of local metallic connection at the asperities (Ref. 2). Electron tunneling effects can occur in aluminum oxide films <10 nm thick under fairly low applied

---

KEY WORDS

Spot Welding
Resistance Welding
Contact Resistance
Electrode Tip
Surface Condition
Plastic Deformation
Ohm's Law
Aluminum Alloys

---

potentials (Refs. 2, 3), but with thicker films, the dielectric breakdown is due to intrinsic and thermal mechanisms that occur at higher potentials (Ref. 3). For both of these cases, the breakdown is accompanied by a rapidly increasing current for a small increase in voltage. Other extraneous surface matter, e.g., lubricants and dirt, diminishes the electrical conducting capacity because it shields asperities from making metallic contact, reducing the total surface contact area of those asperities in metallic contact (Ref. 4). Effectively, the contact resistance is the sum of a low-resistance metallic contact and a high-resistance film contact (Ref. 5).

The contact resistance is a variable of considerable importance in the practical application of electrical resistance spot welding. The contact resistance between the sheets being welded, i.e., the interface resistance of the faying surfaces of the workpiece, is the primary source of ohmic heating for metals such as aluminum, which have high electrical (and thermal) conductivity. Any significant variation in this resistance can affect the process setup parameters and thus the quality of the resultant weld. Thus, the potential for the successful spot welding of aluminum appears to depend upon the nature of the electrical contact at the faying surface (Ref. 6).

In addition to the material resistivity itself, the magnitude of the contact resistance will depend upon the applied load forcing the two surfaces together and the mechanical properties of the materials in contact, since both of these affect the plastic deformation and the load-carrying capacities of the asperities in contact. Because electrical conduction occurs by

metallic contact, the current flow obeys Ohm's law with respect to the applied voltage (Ref. 2). Possible deviations from a linear response can arise from heating effects.

The variability of the as-supplied surface condition of aluminum alloys, mill finish, has led, in the aerospace industry in particular, to the stipulation of prepared surfaces for spot welding by cleaning, etching and other treatments, as defined by specification (Ref. 7). The control of these processes can be monitored by contact resistance techniques, which embody the measurement of the resistance between the sheets under known load conditions, simulating the spot welding setup (Refs. 8–11). Contact resistance specifications are used to assess the suitability of aluminum sheet for spot welding (Ref. 12). Surface treatments, such as conversion coats used to stabilize the aluminum surface for adhesive bonding purposes and lubricants applied to facilitate stamping operations, develop surfaces that display contact resistances orders of magnitude greater than the maximum contact resistance specified by standards (Ref. 12). Evidence is being accumulated that meticulous cleaning operations are not necessary for the successful spot welding of aluminum, that the higher contact resistance developed at the faying surface on uncleaned material can facilitate the welding process and that the contact resistance value does not give an unambiguous measure of the suitability of the aluminum sheet for spot welding (Refs. 12, 13).

Several authors have reported on the contact resistance of aluminum, mild steel, galvanized steel and stainless steel, and its variation with surface condition (Refs. 4, 14–18). In general, the contact resistance decreased with an increase in pressure, following the relationship

$$R_c = C/P^n \qquad (2)$$

where R_c is the contact resistance, P is the pressure, and n and C are constants. In all investigations the considerable variation between nominally identical samples, particularly at lower pressures, was featured. Roberts (Ref. 15) found some effects of rate of load application on the contact resistance of aluminum while Tylecote (Ref. 16) found no correlation between weld strength and initial contact resistance. However, irrespective of its initial value, the contact resistance was found to decrease to approximately the final value during the first quarter cycle of the (AC) resistance welding current (Refs. 4, 15, 16). Studies have been made

of the dynamic resistance changes that occur during the spot welding of galvanized steel (Ref. 19) and HSLA steel (Ref. 20). Gedeon, et al. (Ref. 21), have discussed the problems of obtaining reliable measurements, particularly for the needs of process control. The results of such studies have not been completely incorporated in models of the spot welding process (Refs. 22–28).

The present work has examined the quasi-static and dynamic resistance changes that occur at the faying and electrode workpiece contact surfaces on the passage of an electric current in a variety of aluminum alloys. For these experiments, quasi static and dynamic are defined by analogy with load applications in mechanical testing, viz., quasi static involves an average rate of change of current, dI/dt, ~1 A/s whereas dynamic involves values for dI/dt ~10^7 A/s. Various types of surfaces were examined, including a proprietary conversion coat and lubricant, mill finish, and oxidized and chromate conversion coat. In addition, the contact resistance of uncoated and galvanized steel surfaces was examined for comparison purposes. Finally, the profile of the contact areas on the faying surfaces, which develop as a result of the loading between the two electrodes, was measured.
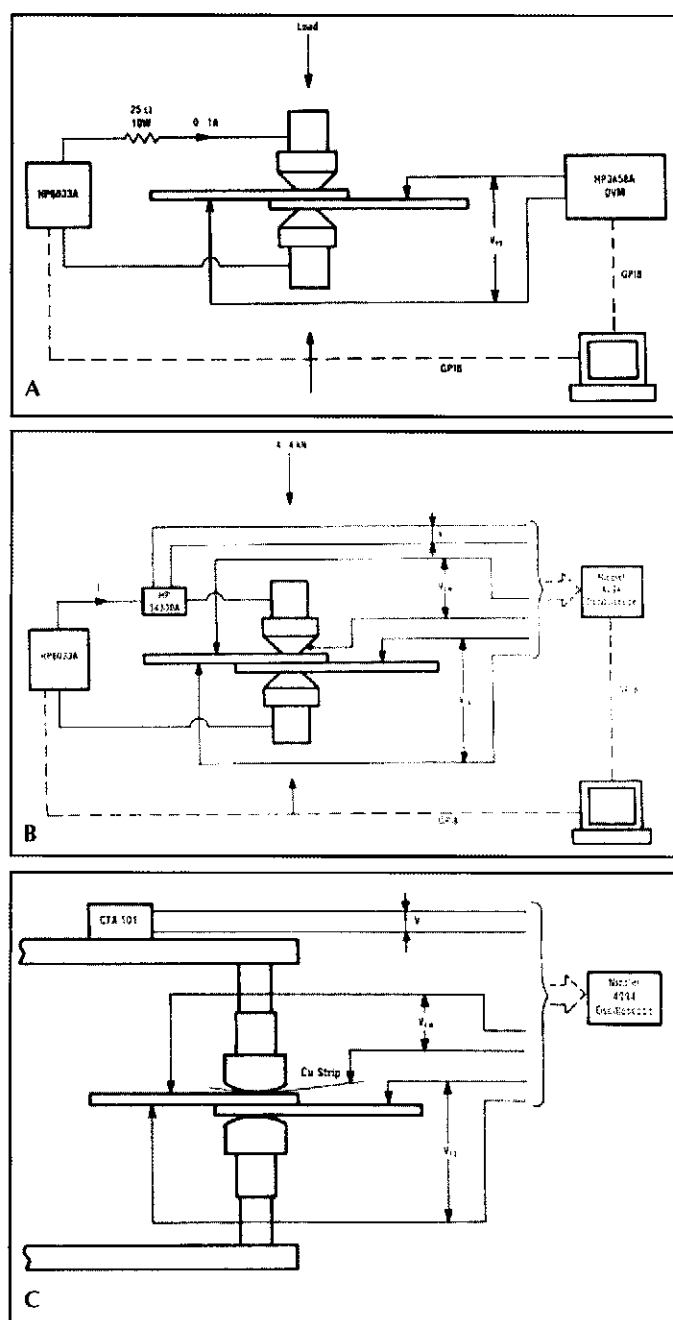
Fig. 1 — A — Experimental arrangement for measuring quasi-static change of contact resistance with change of load; B — experimental arrangement for measuring quasi-static change of contact resistance with change of current; C — experimental arrangement for measuring dynamic change of contact resistance with change of current.

Experimental Procedure

Figure 1A shows schematically the experimental arrangement for the measurements of the change in contact resistance with applied load. Standard spot weld truncated electrode tips with flat ends were mounted on insulated steel supports attached to the top and bottom crossheads of an Instron testing machine.

Fig. 2 — A — Cup and cone profiles on contact surfaces of 0.75-mm AKDQ steel body stock compressed between truncated flat end spot weld electrodes; B — cup and cone profiles on contact surfaces of 1-mm 6111-T4 aluminum compressed between truncated flat end spot weld electrodes.

The sheet samples, 50 x 25 mm (2 x 1 in.), were placed on a micarta loading guide mounted on the bottom electrode at such a height that the samples lay flat and parallel to one another with 25-mm (1-in.) overlap. The jig was constructed so that the top specimen could be lowered onto the bottom specimen without rubbing the two mating surfaces together. The electrodes contacted the sample at the center of the overlap. Current was passed between the electrodes through wires soldered to the electrode tips. Contacts at the electrode/workpiece and faying surfaces were made by means of alligator clips that had one jaw insulated from the specimen. Prior to attaching the clips, a load of ~45 N was applied to the electrode tips. A current of 0.1 A, as recommended by ASTM specification (Ref. 9), was supplied from a Hewlett Packard HP6033A DC programmable power supply with a 25 Ω load resistor in the circuit. Voltages were measured with a Hewlett Packard HP3458A digital multimeter (DVM). A correction was made for the thermal voltages present, by switching off the current after each voltage determination and remeasuring the voltage. Both the power supply and the multimeter were operated under the control of a personal computer (PC) and software. The voltage drop through the electrode spot weld tip was <1 µV. No correction was made for this since it was much less than the other voltages determined. The load was manually changed and the resistance then determined. This sequence was repeated over a series of loads up to a maximum of ~9 kN. Observations were made for both loading and unloading cycles.

The variation of the quasi-static contact resistance with current was deter-

mined after applying a load of 4.4 kN to the electrodes, by incrementally step ramping the output of the DC power supply from ~0.1 A to a maximum <30 A, with an ~1-s interval between each increase to allow the system to stabilize. Figure 1B shows the experimental arrangement. For this experiment, the only load resistance in the circuit apart from the sample was that presented by the current leads. This load resistance was «1 Ω. The current was monitored with a Hewlett Packard HP34330A 30-A current shunt. All voltages were recorded on a Nicolet 4094 digital oscilloscope. The power supply and oscilloscope were controlled by means of a PC and software. Because of switching transients, the power supply was not switched off after each reading to record the contribution of the thermal voltages. It was found that the thermal voltages could make a significant contribution in two cases: 1) at the lower applied current levels for the contact resistance measurements, but not in the current and voltage regions where significant contact resistance changes were observed, and 2) for the bulk resistance measurements of the workpieces between the electrode contacts. For the former, the significance of the observations was not affected, but for the latter, the actual bulk resistances could not be determined.

Dynamic resistance measurements were made in situ on a Taylor Winfield pedestal spot welding machine equipped with a WTC Nadesco controller and recorder. Figure 1C shows the experimental arrangement. Spherical electrode tips with 75-mm (3-in.) radius were used. Sheet samples 70 x 25 mm (2.75 x 1.0

in.) were clamped with 25-mm (1-in.) overlap to a micarta loading guide mounted on the bottom electrode so that the specimens lay flat and parallel with each other. The electrode tip was centered over the overlap and contacted the specimen via a 0.1-mm (0.004-in.) thick strip of copper, which was used for a test lead attachment. This arrangement removed the errors arising from the potential drop generated along the electrode. Voltages at the electrode/workpiece and faying surfaces were determined by means of Kelvin clips attached to the sheet samples and recorded on a Nicolet 4094 digital oscilloscope. The welding current was monitored by an Ohio Semitronics model CTA101 current transducer attached to an arm of the spot welding machine. The output of the CTA101 was also coupled to the Nicolet oscilloscope. The CTA signal conditioner was calibrated using the WTC Nadesco recorder. In all cases, connections between the contact clips and the measurement instrumentation were made by shielded twisted pair conductors, as recommended by Gedcon, et al. (Ref. 21).

The profiles of the contact area on the faying surfaces produced by the loading between the truncated cone electrode tips were determined with a UBM surface-profiling system. In this case, two samples of the sheet material, 25 x 25 mm (1 x 1 in.), fastened together with adhesive tape so that the two pieces could be opened in a book-matched fashion, were mounted on the Instron loading guide and an impression was made by the electrode tips under a load of either 2.2, 4.5 or 6.7 kN. After unloading, the pair of sample sheets was opened,
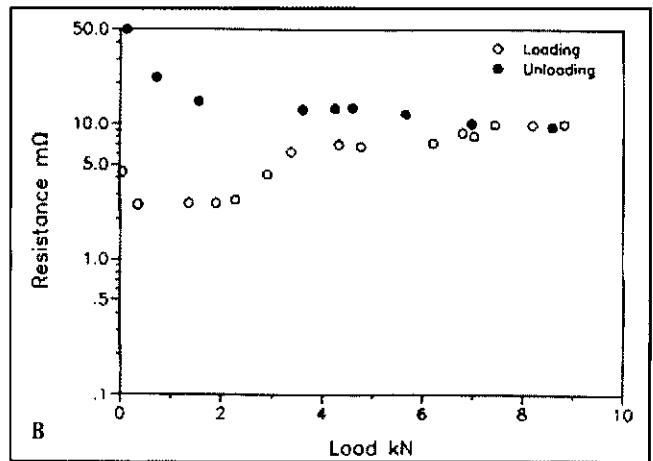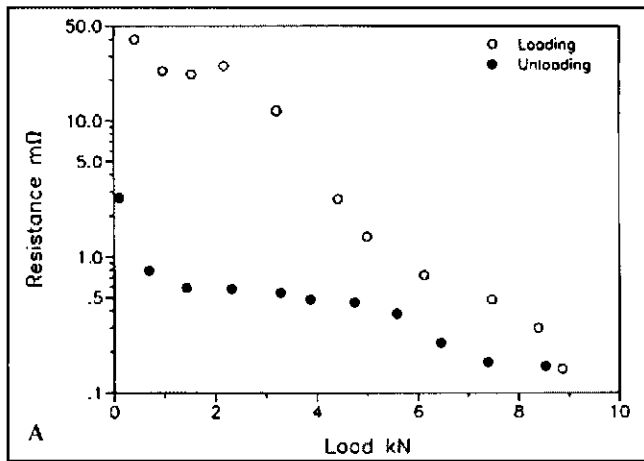
Fig. 3 — A — Variation of contact resistance with applied load for 5754 aluminum alloy with lubricant. Decrease in contact resistance with increase in load on loading, followed by increase in contact resistance on subsequent unloading; B — variation of contact resistance with applied load for 5754 aluminum alloy with lubricant. Increase in contact resistance with increase in load on loading followed by a further increase in contact resistance on subsequent unloading.

mounted on an aluminum block by plasticine and leveled, and a traverse of the faying surfaces was then made on the profilometer. As far as possible, the traverse was made on the corresponding diameters of the contact areas.

Contact resistance and contact profile measurements were made upon various aluminum alloys, 1 and 2 mm (0.04 and 0.08 in.) thick, either in the as-received condition or after annealing to produce a thick oxide film. Similar measurements were made upon two types of body stock steel, 0.75-mm (0.03-in.) AKDQ and 1.1-mm (0.04-in.) galvanized. The materials used are listed in Table 1.

Results

Variation of Contact Profile with Load

Contact profiles were obtained for the AKDQ and galvanized steel and three aluminum alloys, 2024-T3, 6061-T6 and 6111-T4. All contact profiles of the two faying surfaces after loading showed essentially the same result: one of the surfaces displayed a residual depression or cup profile, i.e., it was indented, and the other surface displayed a residual protrusion or cone profile, i.e., it was raised as a result of the plastic deformation caused by the loading between the electrode tips. The most pronounced profiles were developed on the 0.75-mm AKDQ steel subjected to the highest load — Fig. 2A and B. The amplitude of the profile depended upon the applied load, and for this material the maximum amplitudes varied from ~15 to ~35 µm for the 2.2-kN and 6.7-kN loading conditions. Although it cannot be certain that the profilometer traverses were made upon the corresponding diameters, the depth of

the cup always appeared to be greater than the height of the cone. The amplitudes of the profiles were somewhat less for the 1-mm 6111-T4 aluminum alloy. The profiles were barely detectable for the 2-mm 2024-T3 and 6061-T6 alloys loaded to 6.7 kN, the maximum amplitudes being ~1–2 µm. However, profiles could be resolved for the 2-mm 6111-T4 alloy loaded to 4.5 and 6.7 kN, the amplitudes in this case being ~7 µm. In all cases, the amplitude of the asperities within the impressions, i.e., the surface roughness, was reduced but not eliminated by the loading process.

Variation of Contact Resistance with Load

These tests were made upon the 5754 and 5182 alloys, the former having a proprietary chromate conversion coat plus dry-film lubricant and the latter the mill finish. Figures 3 and 4 show typical results for the variation of contact resistance with load for the 5754 and 5182 aluminum alloys, respectively. Contact resistance changes with load were observed, which were both large and highly variable. Most often, the contact resistance changes were well behaved in the sense that a decrease in resistance occurred with an increase in load, as reported by others (Refs. 4, 15, 16, 18, 20). The initial resistance for the 5754 alloy tended toward ~10 mΩ and toward ~100 mΩ for the 5182 alloy. On unloading, the resistance increased to a value less than that observed initially — Figs. 3A and 4A. With a subsequent re-applying of the load, keeping the same specimen in place without removing it from the jig, the resistance change followed the unloading curve values shown in these two figures.

Occasionally, an anomalous response was seen in that on the initial loading cycle, the resistance would increase — Figs. 3B and 4B. On unloading, the resistance increased further, so that the final resistance was appreciably higher than the starting value. On repeating the loading/unloading sequence, the resistance changes became well behaved, the values observed again being at the same level as those of the first unloading curve for a given load.

One experiment was made in which the two sheets of 5182 alloy were separated by one layer of thin plastic film, in which a hole had been cut where the contact was to be made. Figure 5 shows that contact has occurred when a load of 0.9 kN has been applied, and the contact resistance decreases to <1 mΩ for loads >2 kN. On unloading to ~20 N, contact is maintained, indicating that permanent bulk plastic deformation has occurred in the contact zone, as shown in Fig. 2. On

Table 1 — Materials Used in the Experiments

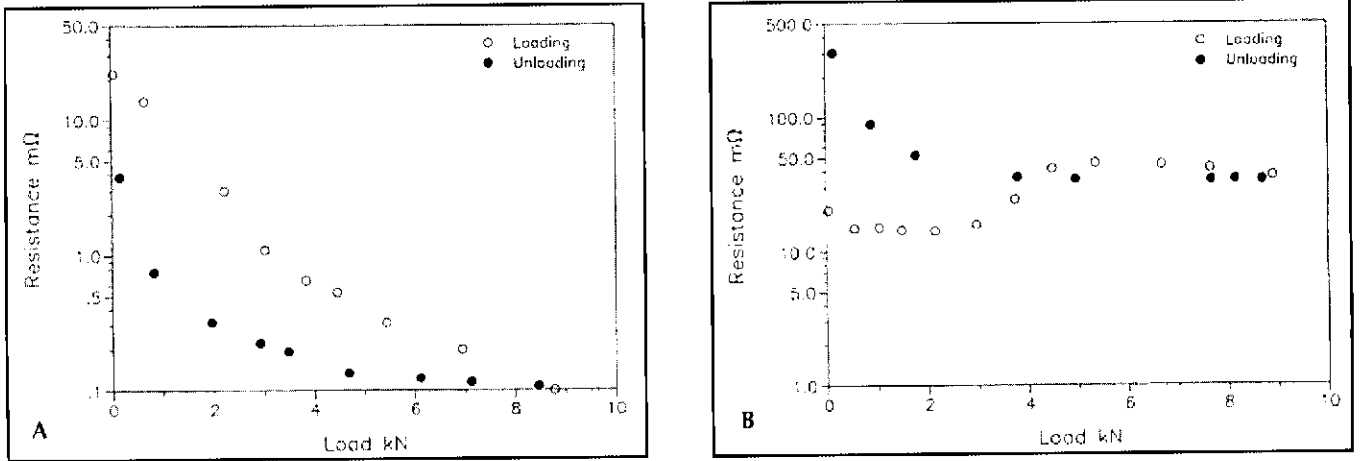| Alloy	Thickness mm	Surface Condition
2024	2.0	Annealed 3h/400°C/ furnace cool
5754	2.0	Proprietary chromate coat, lubricant
5754	2.0	Chromate coat
5182	2.0	Mill finish
6111	1.0	Proprietary chromate coat, lubricant
6111	2.0	Proprietary chromate coat, lubricant
AKDQ steel	0.8	Mill finish
Galvanized steel	1.2	Mill finish

Fig. 4 — A – Variation of contact resistance with applied load for 5182 aluminum alloy with mill finish. Decrease in contact resistance with increase in load on loading, followed by increase in contact resistance on subsequent unloading; B — variation of contact resistance with applied load for 5182 aluminum alloy with mill finish. Increase in contact resistance with increase in load on loading, followed by a further increase in contact resistance on subsequent unloading.

subsequent load cycling, the value of the contact resistance remains in the 5–10-mΩ range.

As shown in Fig. 6, removal of the lubricant does not significantly affect the magnitude of the contact resistance, but a freshly abraded surface has a very low contact resistance, which varies in a well-behaved manner with the applied load.

Quasi-Static Resistance Change with Current

A typical result for the change in voltage across the faying interface of an aluminum alloy, with time, due to the staircase increase in current is shown in Fig. 7. Initially the voltage follows the current increase until it reaches ~0.2 V, when a discontinuity occurs, following which the voltage no longer follows the current

as the current continues to increase. Figure 8 A and B shows the variation of the faying surface resistance with the applied current for samples of the 5754 and 5182 alloys. The discontinuity occurred at an applied current of ~12 A for the 5754 alloy and at ~5 A for the 5182 alloy. After an initial increase, the contact resistance for the 5754 alloy appeared to stabilize at the prebreakdown value with a further increase in the current, whereas, that for the 5182 alloy diminished to a value much lower than that observed prior to the breakdown.

In contrast, the electrode/specimen interface contact resistance was substantially less than the faying surface contact resistance and it remained essentially constant over the same range of applied currents — Fig. 8B. Values for the bulk resistance of the specimen material as measured by the voltage drop between an

electrode and the faying surface could not be determined reliably, presumably because of the thermal voltage effects at the contacts.

No discontinuities were found for contact resistances for the steel for the range of currents, that were available from the power supply.

Dynamic Resistance Change with Current

For these measurements, which were performed using the spot welding equipment, the faying and electrode contact surface resistances for the time span of the spot welding operation, 10 or 12 cycles of 60-Hz current, were calculated using the peak current values only. At these instances in the weld process, the rate of change of the current is zero, so that the inductive component in the im-
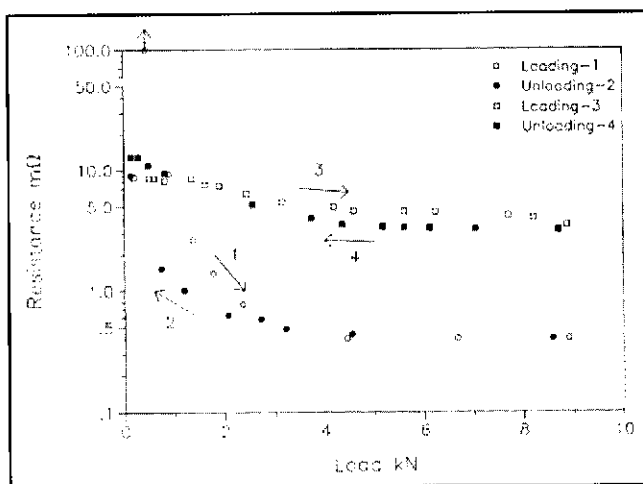

Fig. 5 — Variation of contact resistance with applied load for 5182 aluminum alloy with thin plastic film at faying surface.
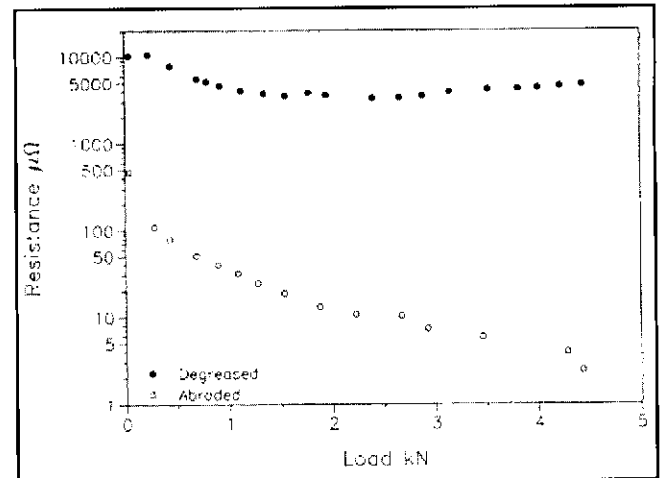

Fig. 6 — Variation of contact resistance with applied load for degreased and abraded 5754 aluminum alloy.

pedance equation,

$$E = IR + LdI/dt \qquad (3)$$

where E is the voltage measured, I is the current, R is the resistance, L is the inductance and t is time, is also zero. The voltage measured is then due only to the resistive component (Refs. 19, 21). In addition, contamination of the signals caused by voltage pickup should also be minimized.

A second calculation of these resistances was made for the first two cycles of the applied current, correcting for the inductive component by empirically eliminating the phase shift between the voltage and current waveforms. The value for L so determined depended upon the particular interface, and also the material between the electrodes, and varied between 1 and 8 nH. Because of the switching transients that occurred near the current crossover points, values for dI/dt were not calculated for those time values that spanned ±0.1 ms over the crossover point times.

Dynamic resistance curves for several aluminum alloys are shown in Fig. 9, and for comparison, similar curves for two types of steel are shown in Fig. 10. In these two figures, the individual values plotted are those calculated for the current maxima or minima, when dI/dt = 0, and the traces are the values calculated using Equation 3. In all cases for the aluminum alloys, irrespective of the original surface condition, it was seen that the initial high contact resistance, ~1 mΩ or more, decreased rapidly until at the first current maximum, i.e., at the first quarter cycle, it reached a value of ~20 μΩ. Over the remainder of the spot welding process, the contact resistance diminished to ~5 μΩ. The contact resistances

at both the electrode/workpiece interface and the faying surface were similar over the whole of the welding cycle.

The dynamic resistance behavior of the body-stock steel, Fig. 10A, was similar to that of the aluminum alloys except that the final resistance values were somewhat higher, ~20 μΩ, and the resistance increased to a maximum after the first quarter cycle indicated by the peak value data, as has been observed by others (Refs. 19, 21). In contrast, the dynamic resistance behavior of the galvanized steel, Fig. 10B, fluctuated much more erratically. The initial resistance was much lower than that of the plain steel, ~100 μΩ, and the faying surface resistance was significantly less than that of the electrode contact resistance.

Discussion

When two sheets are compressed between electrodes as in spot welding, the faying surfaces in the zone surrounding the contact region separate as a result of elastic loading (Refs. 23, 30). Electrical contact is made only across the surface directly in between the electrodes, assuming that there are no other contacts or joining between the two sheets. The metallic contact that is necessary for electrical conduction is achieved simply

by the plastic deformation of the asperities that are in contact and partially support the load (Refs. 1 ,2, 4, 21). This plastic deformation in the asperities causes the oxide film, and any other contaminant film, to rupture. Although the implication is made in finite element models of the spot welding process (Refs. 23, 25–29) that the faying surface interface remains planar, the contact profile results (Fig. 2) indicate that overall plastic deformation of the bulk material occurs at and near the contact surface of the sheets. In addition, there is also the likelihood of relative sliding between the two surfaces in contact. This shows why metallic contact and therefore electrical conduction can be made readily through heavy contaminant layers.

Static Contact Resistance
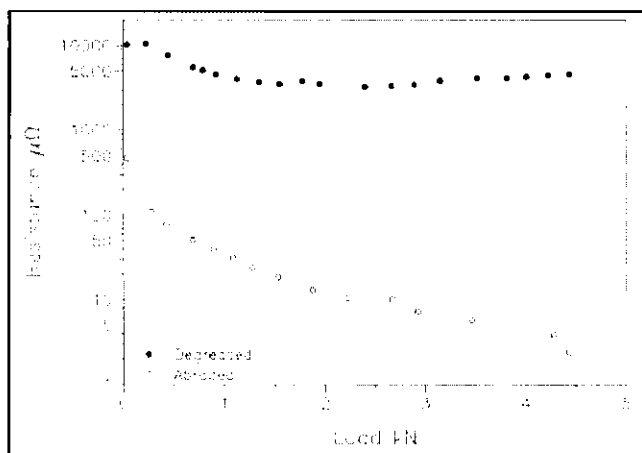
The conducting asperities through

Fig. 7 — Voltage variation across faying interface for 5754 aluminum alloy with chromate conversion coat.
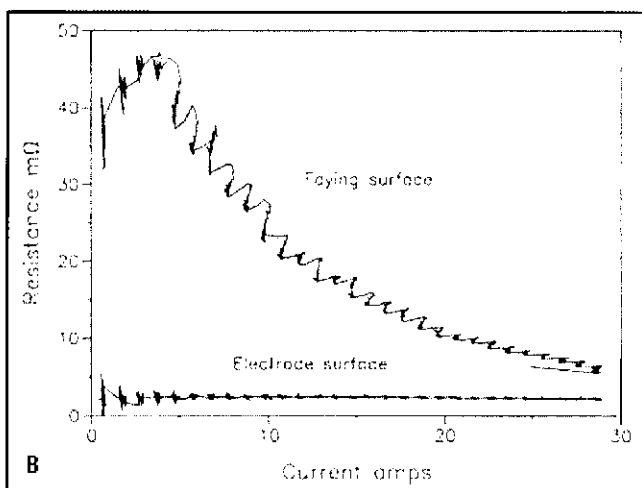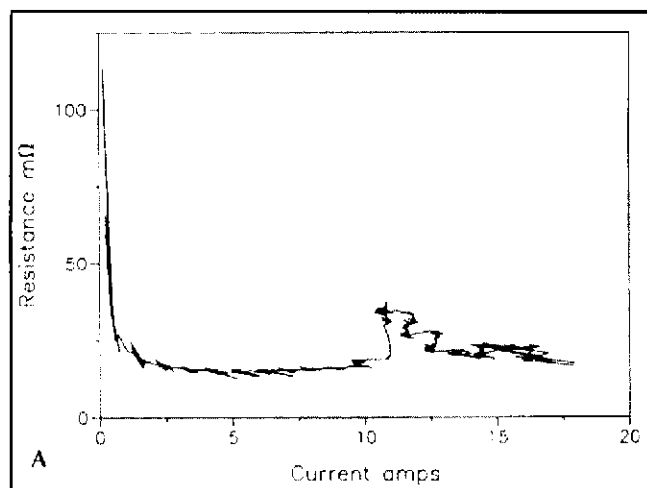

Fig. 8 — A — Variation of faying surface resistance with current for 5754 aluminum alloy with chromate conversion coat; B — variation of resistance across faying surface and electrode/workpiece interfaces with current for 5182 aluminum alloy with mill finish.
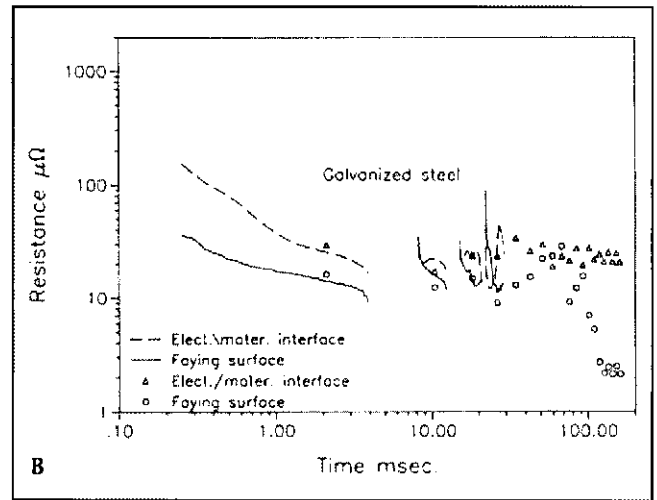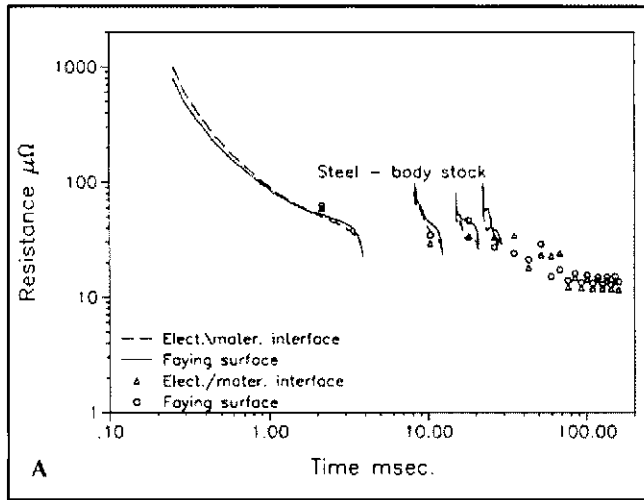
which electrical contact is made initially are small in number and random in distribution (Refs. 4, 20). The load, however, is distributed over these asperities in conduction contact and, in addition, over a much larger number of nonconducting asperities, residual surface contaminant and oxide films, all of which provide additional support (Ref. 4). Similar considerations apply to the electrode/workpiece interface. Although the electrode/workpiece interface involves different metal combinations, unlike the faying surface, which comprises similar metal combinations, its resistance is not necessarily less than that of the faying surface resistance, and as shown in Fig. 10B for the galvanized steel, it can be greater. The probability of more asperities breaking through the contaminant and oxide films and making metallic contact with the copper is not really different. However, these other nonelectrically

conducting asperities and the nonelectrically conducting films, etc., can provide a heat conduction path across the interface. This is an important consideration in understanding the behavior of the contacts in spot welding.

Previous observations (Ref. 20) have demonstrated that the weld nugget forms initially as a toroid around the central axis of the spot weld. This formation was explained on the basis of the heat and electric current conduction profiles generated during the spot welding cycle (Refs. 23, 25, 26). In the extreme, with very high currents, melting will start on the outside of the contact area, as demonstrated for low-carbon steel (Ref. 20). Nugget formation, however, may not commence immediately. Gould (Ref. 22) observed an incubation period of several cycles for the formation of a molten nugget in steel, but in the case of aluminum, a large part of the growth can

have occurred in the first weld cycle (Ref. 14). The genesis of nugget formation, then, is that current transfer across the interface occurs at a few randomly distributed points. These constrictions heat rapidly to temperatures well in excess of the melting point, and the heat diffuses into the bulk metal producing the molten weld nugget. A similar process must occur at the electrode/workpiece interface, but the progression of melting, and alloying of the copper and workpiece metal, i.e., contamination of the electrode, must be greatly restricted by the cooling provided by the electrode. Measurements of contact resistance must therefore be used with care, since static contact resistance is generally associated with solid asperity metallic contact, whereas dynamic contact resistance is associated with molten metallic contact (Ref. 24). In practice, these distinctions are not always made.

Fig. 9 — Dynamic contact resistance A — for 5754 aluminum alloy with proprietary chromate coat and lubricant; B — for 5182 aluminum alloy with mill finish oxide film; C — for 6111 aluminum alloy with proprietary chromate coat and lubricant; D — for 2024 aluminum alloy annealed to produce heavy oxide coat.

Fig. 10 Dynamic contact resistance A — for steel body stock; B — for galvanized steel.

The variation of contact resistance with load is of particular importance with regard to the use of the resistance values in assessing weldability. The present work has shown that, for aluminum alloys, very large variations can be observed, both in magnitude and in the response with change in load, between individual specimens of the same nominal surface characteristics. Similar observations have been reported by Newton (Ref. 12). The well-behaved response previously described (Refs. 4, 15, 16, 18, 20, 24) is that the contact resistance decreases with an increase in load according to some relationship as shown in Equation 2. It was shown (Figs. 4B and 5B) that, for aluminum alloys, the contact resistance can behave in an anomalous manner, by increasing with an increase in load. This response has not been reported before. Probably relative motion occurs at the faying surface, due to the global plastic deformation, and this results in the cup and cone formation, which causes the asperities, initially in metallic contact, to break.

Contact Surface Breakdown

<u>Static Resistance</u>

The present work has shown that when the applied potential across the contact surfaces of two aluminum sheets exceeds ~0.2 V, a discontinuous change in the contact resistance occurs. Changes of this nature are well-known in contact practice because they are related to the breakdown of the surface due to localized fusion, the manifestation being controlled by the applied current. The super temperature, θ, which is the amount by

which the temperature at any point where a constricted electric current flow exceeds that of the bulk, has been related (Refs. 31, 32) to the potential difference U across the constriction by the relation

$$U = \sqrt{a\theta(1+b\theta)} \qquad (4)$$

where the values of a and b depend upon the thermal conductivity and electrical resistivity of the conductor. From Equation 4, the calculated value of U for aluminum is ~0.2 V. This potential was attained when the applied current was ~10 A (Fig. 8) depending upon the nature of the surface preparation. With the power supply available, a breakdown voltage could not be attained with the steel workpieces, due in part to the lower interfacial resistance for the steel as compared to 10–50 mΩ for the aluminum. Holm (Ref. 1) has suggested 0.1 and 0.3 V for the welding potential for aluminum and steel, respectively. Kaiser, et al. (Ref. 20), found, for as-received or cleaned HSLA steel, relatively little variation in the contact resistance with current up to ~100 A but significant decreases with higher currents up to 1000 A. For phosphate-coated HSLA steel, which had a very high initial contact resistance, ~1 Ω, the resistance decreased approximately proportionately to the current. Although Studer (Ref. 4) mentioned that no resistance changes were noted with an aluminum alloy for applied currents between 0.1 and 20 A, the present work has shown that a breakdown of the surface can occur with currents less than 20 A, although the observed resistance may not change significantly as a consequence.

Practice has shown that aluminum sheet, displaying contact resistances

greatly exceeding those stipulated in generic standards, e.g., the German standard DVS2929, can be welded satisfactorily (Ref. 12). However, static resistance values for aluminum alloys have not been found to correlate well with weldability or electrode life (Refs. 13, 33). The criterion for weldability used here is that 2000 consecutive welds can be made without the necessity of dressing electrodes or without modifying weld schedule parameters (Ref. 34). These conclusions were reached using resistance tests that employed currents of 10–100 A; resistance values ~1 mΩ were reported. Rivet and Lucas (Ref. 33) also used a modified spot welding cycle with a current of 10 kA and found that the surface resistance was ~100 $\mu\Omega$. ASTM specification (Ref. 9) suggests a power supply circuit with a maximum 20 mV open circuit voltage and 100 mA short circuit current for the dry circuit testing of contacts to avoid spurious readings caused by oxide film breakdowns, etc. The current values recommended for determining the contact resistance of aluminum vary widely. A welding handbook (Ref. 8) suggests a current of 30 mA, a German specification (Ref. 10) requires 10 A and an early G.M. specification (Ref. 35) required 70 A. An in-house device used for the screening of aluminum sheet for production stampings uses a current of 100 A (Ref. 36).

The present work has shown that, with aluminum, breakdown of the surface can start at currents of ~5 A so that if currents of this magnitude or higher are used then a surface is being examined on which some fusion may have already started. This fusion effectively represents the initial stages of the formation of the weld button. The static resistance values

reported in the present work were obtained with a current of 0.1 A, as suggested by the ASTM specification (Ref. 9), and the values obtained, ~10 mΩ, were significantly larger than those reported by Rivet and Lucas (Ref. 33) and Pickett and Griffore (Ref. 13). Newton (Ref. 12), in tests to the German DVS2929 specification (Ref. 10), but using a current of 3.3 A, has also observed contact resistances ~10 mΩ. Thus, low currents, <5 A, will apparently give much higher contact resistance values than when higher currents are used, i.e., breakdown of the surface has not occurred.

Dynamic Resistance

The observations on the dynamic resistance changes with weld time are similar to those noted by many others (Refs. 4, 6, 16, 17, 19, 20). Essentially, all the resistance change occurs in the first quarter cycle of the applied current, and the faying surface resistance is approximately 10 µΩ on completion of the weld cycle for aluminum and 30–40 µΩ for steel. Because of signal noise, the minimum time at which a measurement could be made after the current was switched on was 0.2 ms, at which point the current flowing was already ~1500 A. Thus, the changes in the surface mentioned previously, caused by currents greater than a few amperes, have already occurred by the time these particular measurements can be made, i.e., fusion has already occurred (Ref. 24). However, at this point, the contact resistance is still high, ~1 mΩ, a value that can be compared with the quasi-static resistance 10–20 mΩ, measured at ~30 A current — Fig. 8B and C. The dynamic resistance for the steel followed similar changes, although the values for the galvanized steel were significantly lower; Savage, et al. (Ref. 19), has noted similar changes. Gedeon, et al. (Ref. 21), has observed that changes in dynamic resistance that are measured between the electrodes rather than at the individual interfaces may be due more to effects occurring at the electrode interface rather than at the faying surface. These observations are not confirmed by the present work or by Tylecote (Ref. 16). Lee and Nagel (Ref. 24) indicate that the electrode/workpiece resistance may be appreciably higher than that of the faying interface, and the present work also has indicated that it can be higher or lower than that of the faying surface.

It is seen in Figs. 9 and 10 that, during the first two cycles of weld current, the calculated faying surface and electrode/workpiece resistances at the start of

each half cycle after the first half cycle are greater than the values of the resistance at the end of the previous half cycle. Tylecote (Ref. 16) has also noted similar effects, which were associated with the alternating direction of the current flowing. In this first part of the weld cycle, the voltages detected at these two interfaces are considerably distorted from a sinusoidal form, indicating that both L and R in Equation 3 are varying over each quarter cycle of the weld current as the weld nugget forms and grows. Calculations of the interface resistances, made by assuming that the values of L and R were the same over two consecutive samples of data, reduced the differences between the resistance at the end of each half cycle and that at the start of the following half cycle but introduced a considerable degree of scatter in the resistance curve.

The bulk resistance of the workpiece as derived from the dynamic resistance tests was <0.5 µΩ for steel and <0.05 µΩ for aluminum. Although the experimental waveforms for these measurements did show the effects of coupling from the welder secondary circuit (Ref. 15), the calculated values were derived from the voltages at the current maxima and minima, when the induced voltages should have been zero. The observed values are significantly less than those quoted by Lee and Nagel (Ref. 24), ~50 µΩ for steel at the end of 10 cycles of welding current. While some objection can be made to their estimation, which includes the assumption that the faying surface contact resistance is zero after only ~2 cycles of welding current, the present results may be in error because of the influence of thermal voltages. The influence of the thermal voltages may be the cause of the cyclic effect seen in Fig. 10 for the faying and electrode surface resistances toward the end of the weld cycle. Because the dynamic resistance tests were made with alternating current, the thermal effects are alternately cancelled and added, giving the cyclic waveform shown.

Power Dissipation during Welding

All models of the spot welding process to date have ignored the contact resistance and instead have assumed that the Joule heating is caused by the bulk resistance. Some distinctions must now be made between the bulk resistance and resistivity of the solid and the bulk resistance and resistivity of the liquid. Furthermore, the electrode/workpiece contact resistance can be of the same order of magnitude as that of the faying interface. It is incorrect to assume, as has been

stated in the German DVS2929 specification (Ref. 10), that the electrode contact resistance can be determined by bringing the tips together without any intervening workpiece. This gives a copper-copper interface contact resistance, when what is really needed is a copper-aluminum interface resistance.

The observed contact resistance changes have a significant effect upon the current signature and the consequent power variation during a spot weld cycle. It is found that the current waveform for the first two cycles of current increases in amplitude as the resistance at the contact surfaces decreases. Calculations of the power dissipated at these surfaces indicate that the peak power input occurs during the second cycle. Only about one-third of the power dissipated actually causes welding. If the present results are correct, the bulk resistance measured in these experiments is that of the solid, and for the aluminum alloys, the heat input generated by this solid bulk resistance is two orders of magnitude smaller than that provided by the interface resistance. Even for steel, the solid bulk resistance does not contribute significantly to the total heat input. It must be remembered that as soon as appreciable current has started to flow, causing fusion at the faying surface, the nature of the interface has essentially changed, and the faying surface interface resistance is now due to the bulk resistivity of the fused metal in the constricted contact zone lying between the two electrodes. From Figs. 9 and 10, the bulk resistance of the fused metal for the steel is about three times that for the aluminum. Thus, the major difference in the spot welding process between aluminum and steel, the need for much higher welding currents for aluminum, could be ascribed to the lower thermal conductivity and specific heat of steel relative to aluminum and the higher bulk resistance of the fused metal in the steel.

Constriction and Asperity Fusion

The effects described above can be explained if it is assumed that surface resistance is not a material property, as is bulk resistivity, but is a specimen characteristic that can be modified readily by the tools with which it is being examined. The factors that give rise to surface resistance have been well described (Ref. 1). The resistance effects described above can be more readily explained on the basis of metallic contact formation rather than to the formation and breakdown of an insulating oxide layer. This is most readily seen from results such as those
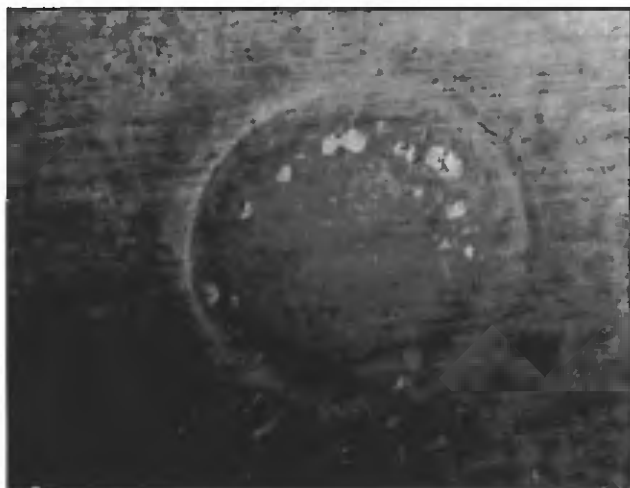
Fig. 11 — Faying surface of spot weld made at 7.1 kN, 8 cycles 32 kA RMS current (12X).

shown in Fig. 7. Before the breakdown voltage of ~0.2 V is attained, the slope of the voltage/time curve is seen to be both positive and increasing. Because the current was being incremented in constant steps, this implies that metallic conduction was involved, with a positive temperature coefficient of resistivity. If the conduction had been due to oxide film breakdown, because of the cumulative nature of this, the slope of the voltage/time curve would have decreased.

The random profile of surfaces is well-known. Patrick, et al. (Ref. 6), for example, shows surface roughness profiles for different aluminum alloy finishes. Surface contact primarily is made via a few asperities, which have broken through any surface oxide film, or other contamination because of plastic deformation (Refs. 4, 24). The extent of plastic deformation depends upon the load and geometry of the contacting surfaces. It may be limited to just the few asperities in contact, or as has been shown in the present work, bulk plastic deformation can have occurred with possibly sliding between the surfaces in contact. It is probably incorrect to assume that all the load is supported just by the asperities in contact since the surface films, both oxide and contaminant, may also provide load-bearing capability. The surface resistance then arises from the bulk resistivity provided by the few asperities in metallic contact as described by Holm (Ref. 1), Equation 1. For aluminum alloys, if the contact resistance is ~10 mΩ, the value for r is ~2.5 μm. The value for R_c could increase or decrease with applied load as shown in the present work, due to the few metallic contacts breaking under the sliding and bulk plastic deformation or more being formed, as the case

may be. The actual value for R_c thus depends upon a statistical probability of contacts occurring in a given place (Ref. S). A current of 5–10 A is sufficient to raise the temperature of the constriction to its melting point. This is the start of nugget formation. Once fusion starts, the contact resistance immediately starts to diminish and soon falls to values ~20 μΩ.

The action of electrode force may be more clearly understood in the light of the constriction formation. An increase in load has been considered to increase the contact area and reduce the current density at the faying surface (Ref. 28), which results in smaller nuggets. Smaller nuggets as a result of an increase in electrode load have also been observed by Thornton, et al. (Ref. 37). Pickett and Griffore (Ref. 13) have observed that an increase in weld force produces an increase in electrode life. However, it is not thought that a reduced current density at the faying surface is responsible for these effects. As shown in Figs. 3 and 4, changes in load above a certain level do not produce significant further differences in contact resistance. These observations, which were made on the faying surface, must apply also to the electrode contact surface. Figure 9 indicates that the electrode contact resistance is as significant a source of heat as is the faying surface contact resistance. The faying surface of a spot weld made with an applied load of 7.1 kN is shown in Fig. 11. This is an extreme case of a failed spot weld, but it illustrates that initial electrical contact is made in just a few places over the nominal contact surface. These actual contact places are located along a zone near the base of the cup, and the corresponding lip of the cone, of the cup and cone formation previously described. Similar, possibly random, distributions of a few electrical contact points must exist at the electrode interface, so that a load increase will not change significantly the electrical characteristics of this interface. However, the load increase must increase the thermal conductivity of this interface. Unlike the electrical current, heat is conducted across the entire interface, not just the points of metallic contact. Thus, a load increase extracts more heat from the faying surface, which

results in smaller nuggets, and improves the cooling of the electrode contact surface, resulting in longer electrode life.

Conclusions

The electrical contact resistance of aluminum alloys can cover a very wide range of values in magnitude. The decrease in contact resistance, which usually occurs with an increase in the load on the contact for other metals, may not occur with aluminum alloys that are typical of those used in the automotive industry. Plastic deformation occurs in the region of the workpiece under the electrode tips, which results in the development of a protrusion profile (cup) in the one piece and a depression profile (cone) in the other piece in the contact zone of the faying surface.

Electrical conduction through the contact surfaces is by metallic conduction rather than by oxide film breakdown. Surface changes involving local fusion can occur in making contact resistance measurements with currents, which are significantly greater than 1–2 A. These changes can give values for the contact resistance that are much lower than those obtained with currents ~0.1 A. Contact resistance measurements on aluminum alloys should be performed in accordance with ASTM guidelines.

Dynamic resistance changes probably are of little significance for monitoring the progression of spot weld growth for aluminum, since the majority of the resistance change occurs in the first quarter cycle of the weld current application. Peak welding power is developed in the second half cycle of welding current. A welding schedule that is too short could introduce an excessive heat input that could shorten weld tip life. The electrode/workpiece interface resistance is significant, of the same magnitude as the faying surface resistance, and follows the same changes with time as the faying surface resistance.

References

1. Holm, R. 1967. *Electric Contacts*, New

York, N.Y., Springer-Verlag.

2. Jones, F. L. 1957. *The Physics of Electrical Contacts*, Oxford, U.K., Clarendon Press.

3. Wefers, K., and Misra, C. 1987. Oxides and hydroxides of aluminum. Alcoa Technical Paper No.19, Revised, New Kensington, Pa., Alcoa Laboratories.

4. Studer, F. J. 1939. Contact resistance in spot welding. *Welding Journal* 18(10): 374-s to 380-s.

5. Greenwood, J. A. 1966. Constriction resistance and the real area of contact. *Brit. J. App. Phys.* 17: 1621-1632.

6. Patrick, E. P., Auhl, J. R., and Sun, T. S. 1984. Understanding the process mechanisms is key to reliable resistance spot welding aluminum auto body components. *Trans. SAE.* 93: 1-14.

7. *Military Specification: Welding, Resistance, Spot and Seam.* DOD MIL-W-6868D 3/28/78.

8. *Welding Handbook*, Vol. 4, 7th ed., American Welding Society, Miami, Fla.

9. B539-80 1985. *Standard Test Methods for Measuring Contact Resistance of Electrical Connections.* Philadelphia, Pa., ASTM.

10. DVS2929 August 1985. *Resistance Welding — Measuring the Transitional Resistance on Aluminum Work Materials*, Deutscher Verbond fur Schweisstechnik e.V., Düsseldorf, Germany.

11. DVS2929 March 1988. *Notes for the Areas of Application of Single Sheet Measurement and Double Sheet Measurement in Aluminum Materials.* Amendment to DVS2929 August 1985. Deutscher Verbond fur Schweisstechnik e.V., Düsseldorf, Germany.

12. Newton, C. J. 1993. Alcan International Ltd., Banbury, U.K. Private communication.

13. Pickett, K. M., and Griffore, H. J. 1994. Ford Motor Co., Dearborn, Mich. Private communication.

14. Auhl, J. R., and Patrick, E. P. 1994. A fresh look at resistance spot welding of aluminum automotive components. Paper No. 940160, *SAE Inter. Congress and Exposition*, Detroit, Mich.

15. Roberts, W. L. 1951. Resistance variations during spot welding. *Welding Journal* 30(11): 1004-s to 1019-s.

16. Tylecote, R. F. 1941. Spot welding, part II: contact resistance. *Welding Journal* 20(12): 591-s to 602-s.

17. Savage, W. F., Nippes, E. F., and Wassell, F. A. 1977. Static contact resistance of series spot welds. *Welding Journal* 56(11): 365-s to 370-s.

18. Vogler, M., and Sheppard, S. 1993. Electrical contact resistance under high loads and elevated temperatures. *Welding Journal* 71(6): 231-s to 238-s.

19. Savage, W. F., Nippes, E. F., and Wassell, F. A. 1978. Dynamic contact resistance of series spot welds. *Welding Journal* 57(2): 43-s to 50-s.

20. Kaiser, J. G., Dunn, G. J., and Eagar, T. W. 1982. The effect of electrical resistance on nugget formation during spot welding. *Welding Journal* 61(6): 167-s to 174-s.

21. Gedeon, S. A., Sorensen, C. D., Ulrich, K. T., and Eagar, T. W. 1987. Measurement of dynamic electrical and mechanical properties of resistance spot welds. *Welding Journal* 66(12): 378-s to 385-s.

22. Gould, J. E. 1987. An examination of nugget development during spot welding, using both experimental and analytic techniques. *Welding Journal* 66(1): 1-s to 10-s.

23. Nied, A. 1984. The finite element modeling of the resistance spot welding process. *Welding Journal* 63(4): 123-s to 132-s.

24. Lee, A., and Nagel, G. L. 1988. Basic phenomena in resistance spot welding. Paper 88027, *SAE Inter. Congress and Exposition*, Detroit, Mich.

25. Tsai, C. L., Dai, W. L., Dickinson, D. W., and Papritan, J. C. 1991. Analyis and development of a real-time control methodology in resistance spot welding. *Welding Journal* 69(12): 339-s to 351-s.

26. Tsai, C. L., Jammal, O. A., Papritan, J. C., and Dickinson, D.W. 1992. Modeling of resistance spot weld nugget growth. *Welding Journal* 70(2): 47-s to 54-s.

27. Gould, J. E. 1994. Modelling primary dendrite arm spacings in resistance spot welds. part I — modelling studies. *Welding Journal* 72(4): 67-s to 74-s.

28. Browne, D. J., Chandler, H. W., Evans, J. T., and Wen, J. 1995. Computer simulation of resistance spot welding in aluminum. part I. *Welding Journal* 74(10): 339-s to 344-s.

29. Browne, D. J., Chandler, H. W., Evans, J. T., James, P. S., Wen, J., and Newton, C. J. 1995. Computer simulation of resistance spot welding in aluminum. part II. *Welding Journal* 74(12): 417-s to 422-s.

30. Civelek, M. S., Erdogan, F., and Cakiroglu, A. O. 1978. Interface separation for an elastic layer loaded by a rigid stamp. *Int. J. Engr. Sci.* 16: 669-679.

31. Kohlrausch, F. 1900. About the stationary temperature condition of an electrically heated conductor. *Ann. Phys. Lpz.* 1:132-158.

32. Bowden, F. P., and Williamson, J. P. B. 1958. Electrical conduction in solids I: influence of the passage of current on the contact between solids. *Proc. Roy. Soc.* 246A: 1-12.

33. Rivet, R. M., and Lucas, W. 1983. Joining aluminum for mass production industries. *Trans. SAE.* 93: 1-16.

34. Dilay, W., Rogala, E. A., and Zulinski, E. J. 1977. Resistance welding aluminum for automotive production. Paper No. 770305, *SAE Inter. Congress and Exposition*, Detroit, Mich.

35. G.M. Standards, *Surface Resistance Measurement for Aluminum Spot Weld Cleaning*, G.M. 4403-P, July 1952.

36. Dolphi, J. W. 1994. Ford Motor Co., Dearborn, Mich. Private communication.

37. Thornton, P. H., Krause, A. R., and Davies, R. G. 1994. Ford Motor Co., Dearborn, Mich. Unpublished research.